

Neutronic Design Studies on Small Accelerator ^7Li (p, n) Neutron Sources for Neutron Scattering Experiments

Fujio Hiraga, Takanori Okazaki and Yoshiaki Kiyonagi
*Graduate School of Engineering, Hokkaido University, Kita-13, Nishi-8, Kita-ku,
Sapporo, 060-8628, Japan*

ABSTRACT

^7Li (p, n) reaction by the protons having an energy near the threshold energy gives lower energy neutrons than the other reactions such as a photo-neutron source and will enable us to make a compact neutron source. We have performed optimum studies on a cold neutron source based on the ^7Li (p, n) reaction and compared the efficiency of the cold neutron source with other ones based on different reactions. It turned out that the cold neutron source using the ^7Li (p, n) reaction using 2.5 MeV protons is most efficient and a very compact system can be realized.

1. Introduction

With the growing need for various applications using neutrons such as the nondestructive inspection in industrial use, the boron-neutron capture therapy in medical treatment and the technology to detect a hidden nuclear material in homeland security, the necessity for small accelerator-based neutron sources is increasing. Recently, a 3 m long proton linear accelerator with a weight of 2.7 t has been developed.[1] This can emit protons with energy up to 3 MeV under the condition of 100 pulses per second, 100 μs pulse width and 1 mA beam current, and the light weight and the compact size make it easily to transport.

About $1 \times 10^{12} \text{ s}^{-1}$ neutrons with energies up to 800 keV can be generated by using a ^7Li target combined with a proton linear accelerator emitting 2.5 MeV protons at current of 1 mA.[2] The lower energy neutrons created by the ^7Li (p, n) reactions than those from the ^9Be (p, n) and the Bremsstrahlung (γ , n) reactions may increase an efficiency of moderation in a moderator and decrease shielding required for a facility. Thus a cold neutron source based on the ^7Li (p, n) reactions allows flexibility for installation in any facility with a low construction cost and is very useful for wide fields of material research using cold neutron scattering experiments. The ^7Li neutron source will have capability to be used in many places in manner of a moving trailer and may also promote the use of neutrons for technologies in homeland security.

For the development of the compact and usefull neutron source for neutron scattering experiments, we have designed a cold neutron source equipped with a Li target and a proton linear accelerator with the proton energy of 2.5 MeV and the beam current of 1 mA. In the case of the ^7Li (p, n) reactions caused by protons with an energy of 2.5 MeV, the yield of neutrons from a thick target peaks in the angle of 40 degree with respect to the direction of the initial protons. [3] We thus studied the ^7Li (p, n) cold neutron source using two calculation models with different configurations between a Li target and a cold the

neutronic performance of the moderator. Furthermore, we compared the neutron fluxes from the ^7Li (p, n) cold neutron sources with those from the ^9Be (p, n) and the Bremsstrahlung (γ , n) cold neutron sources to reveal the effects of the energy and angular distributions of source neutrons on the neutron fluxes. In the calculations, the scattering and absorption of neutrons in the structure materials and the neutron streaming in the channels around the moderator were taken into account.

For the design of shielding components, the yields and the energies of particles from the Li target bombarded with 2.5 MeV protons of 1 mA current must be taken into account. The fact that the ^7Li (p, n) reactions generate neutrons with energies up to 800 keV suggests that light materials including hydrogen as the shielding components must be most effective for the neutrons; however, photons with an energy of 14MeV or higher energies accompanying with the ^7Li (p, n) reactions necessitate heavy materials as the shielding components for the photons. We thus separately designed the shielding components for neutrons and γ -rays to reduce the volume of shields around the ^7Li (p, n) cold neutron source.

Here, we present the optimization studies on the cold neutron source using the ^7Li (p, n) reaction as well as other reactions, the shielding design, and finally discuss the compactness of this neutron sources.

2. Calculation method

2.1. Calculation models for examining neutronic performance

Figure 1 and 2 show the calculation models for examinations of neutronic characteristics of the ^7Li (p, n) cold neutron source. The major parts are a Li target, a 22K methane moderator, a polyethylene pre-moderator and a beryllium reflector. The duct for protons is aligned with or perpendicular to the duct for neutrons in the cases of the S-type and the L-type, respectively. The distance from the Li target to the moderator surface was set at 6cm for both S-type and L-type. The two models have different configurations between the Li target and the moderator, *i.e.* the difference in the thickness of methane in the direction of the initial protons, which is 10 cm for the L-type and 2.5 cm for the S-type respectively.

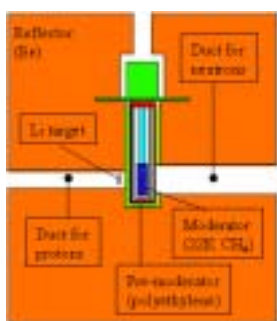


Fig. 1 Longitudinal section of the calculation model of the S-type cold neutron source

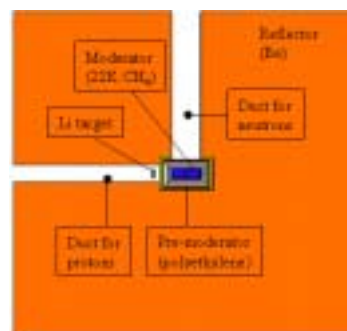


Fig. 2 Cross section of the calculation model of the L-type cold neutron source

Figure 3 shows the detailed structure around the moderator for the L-type. A 0.01 cm thick lithium foil installed on a copper can of 3 cm diameter and 0.5 cm thickness having a

0.1 cm thick water layer was bombarded with 2.5 MeV protons in a beam of 1 mA current. The proton energy drops just below 1.88 MeV during a passage through the 0.01 cm thick lithium foil, which is the threshold energy of the ${}^7\text{Li}$ (p, n) reactions. The 0.01 cm thick lithium foil was thus chosen to minimize the generations of disturbing photons of 478 keV by the ${}^7\text{Li}$ (p, p γ) reactions. The structure materials such as the methane vessel, the shield for heat and the outer vessel are made of aluminum alloy and are separated by a shortest distance of 0.9 cm. The thickness of the rectangular parallelepiped moderator (t_m), the pre-moderator (t_p) and the reflector (t_r) were examined parametrically. The bombardment of the lithium foil by protons with an energy of 2.5MeV and a current of 1mA yields neutrons of $8.8 \times 10^{11} \text{ s}^{-1}$ having an average energy of 326 keV.[3] The energy spectra and the angular distributions of neutrons caused by ${}^7\text{Li}$ (p, n) reactions were calculated by the computer code LIYIELD[3] and used as a source term for the computer code MCNPX.[4] For the S-type and the L-type of the cold neutron sources, the neutron fluxes at a distance of 5 m from the moderator were calculated by the MCNPX.

We also examined the neutronic performance of the simplified models excluding the structure materials in order to estimate the optimal dimensions of the moderator, pre-moderator and reflector. **Figure 4** shows the simplified model for L-type. In this model, a 0.01 cm thick lithium target is installed on the pre-moderator.

In order to study the efficiency of each neutron production reaction as a cold neutron source, we calculated the neutron fluxes from the S-type and the L-type of the ${}^9\text{Be}$ (p, n) and the Bremsstrahlung (γ , n) cold neutron sources, where the 0.01 cm thick lithium foil was replaced by a 0.1 cm thick beryllium foil or a 1 cm thick tungsten foil and it was assumed that the ${}^9\text{Be}$ (p, n) or the Bremsstrahlung (γ , n) reactions occur in the foil. We used the energy spectra and the angular distributions of neutrons from ${}^9\text{Be}$ (p, n) reactions caused by protons with an energy of 11 MeV[5] and the isotropic evaporation neutrons given by the MCNPX in the case of the Bremsstrahlung (γ , n) reactions caused by electrons with an energy of 35 MeV.

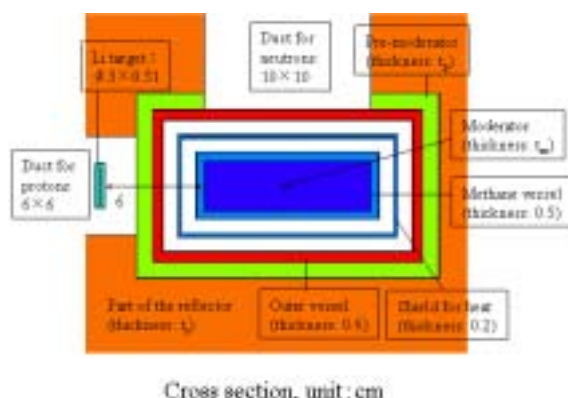


Fig. 3 Detailed structure around the moderator for the L-type source

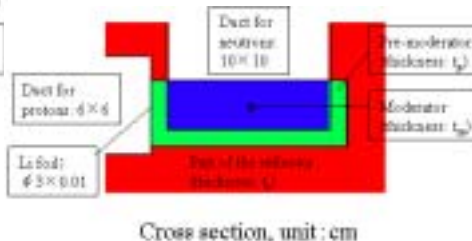


Fig. 4 Detailed structure around the moderator for the simplified L-type source

Figure 5 and 6 show the energy spectrum ($dY(E)/dE$) and the angular distribution ($dY(\theta)/d\theta$) of neutrons from the Li target bombarded by 2.5 MeV protons. They were estimated by using a geometry where the Li target was placed in the center of a sphere with a radius of 100 cm and the neutron flux per single neutron production at the sphere surface was tallied by the MCNPX: the angular distribution of neutrons was obtained by

multiplying the neutron flux by the $2\pi \sin \theta$ term from the solid angle differential element. Here, θ is the polar angle to the direction of the initial protons. The energy spectra and the angular distribution of neutrons produced by the reactions of the ${}^7\text{Li}$ (p, n) with 2 MeV protons, the ${}^9\text{Be}$ (p, n) with 11 MeV protons and the Bremsstrahlung (γ , n) with 35 MeV electrons are also calculated and shown for comparison. From Fig. 5, it is found that the maximum energy of neutrons from the target increases with the increase in the energy of the initial particles. From Fig. 6, it is indicated that that the peak around the polar angle of 40 degree decreases with the increase in the energy of protons in the case of the (p, n) reactions; the distribution curve for the Bremsstrahlung (γ , n) reaction deviates from an isotropic angular distribution of a symmetrical function, since neutrons with the direction of emission of less than 90 degree decrease in numbers during the passage through the target materials.

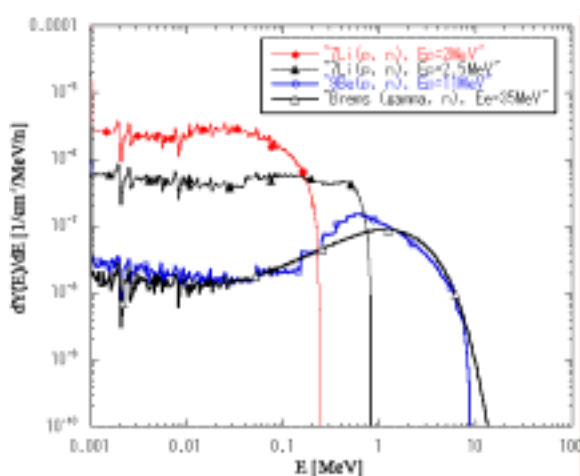


Fig. 5 Neutron energy spectra per neutron production from various targets

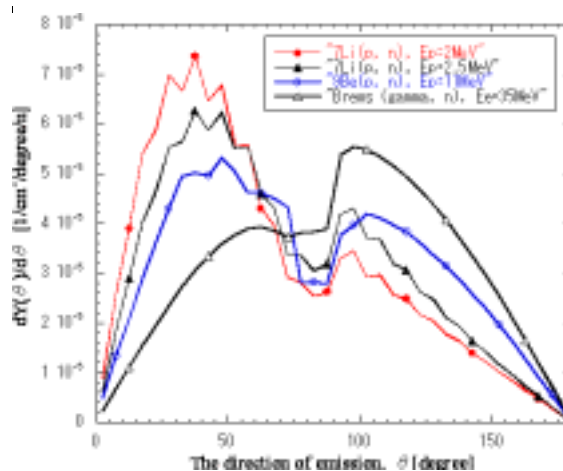


Fig. 6 Neutron angular distribution per neutron production from various targets

2.2. A method for designing the shielding components

Considering the slowing-down length of neutrons produced by the ${}^7\text{Li}$ (p, n) reactions with $E_p=2.5\text{MeV}$ in hydrogenous materials are shorter than that of the evaporation neutrons, we should use a material including hydrogen and absorbent elements for thermal neutrons as the shielding components. For dropping the volume of shields around the ${}^7\text{Li}$ (p, n) cold neutron source, we adopted shields with two layers consisting of the inside lead slabs for the energetic photons and the outside boric acid resin slabs for the neutrons with energies up to 800 keV. The boric acid resin slab (1.33 g/cm^3 density) is used as the shielding components for neutrons in the Hokkaido University 45MeV LINAC and contains H ($4.71 \times 10^{22} \text{ cm}^{-3}$), B ($9.04 \times 10^{21} \text{ cm}^{-3}$), O ($2.96 \times 10^{22} \text{ cm}^{-3}$), etc. A case where the iron slabs or the boron-enriched concrete slabs are used for the shielding components was also examined for comparison. The boron-enriched concrete slab (2.2 g/cm^3 density) is used as the shielding components for neutrons in the J-PARC MLF and contains H ($2.49 \times 10^{22} \text{ cm}^{-3}$), B ($1.54 \times 10^{21} \text{ cm}^{-3}$), O ($4.25 \times 10^{22} \text{ cm}^{-3}$), etc.[6] We aimed at reduction of the surface photon and neutron dose on the shielding components down to $10 \mu\text{Sv/h}$ respectively, since a 2.5 MeV proton linear accelerator having the surface radiation dose of less than $20 \mu\text{Sv/h}$ on the shielding components is permitted by the regulation in Japan to be used anywhere. We also examined the shielding components of the Bremsstrahlung (γ , n) cold neutron source for comparison.

ICANS XIX,
19th meeting on Collaboration of Advanced Neutron Sources
 March 8 – 12, 2010
 Grindelwald, Switzerland

As an initial neutron source for the calculations of the surface radiation dose, we used the energy spectra and the angular distributions of neutrons mentioned above and used the isotropic photons from the ${}^7\text{Li} (p, n) {}^7\text{Be}$, ${}^7\text{Li} (p, p) {}^7\text{Li}$ and ${}^7\text{Li} (p, \alpha) {}^4\text{He}$ reactions caused by 2.5 MeV protons and the Bremsstrahlung caused by 35 MeV electrons. **Table 1** shows the energies and the yields of photons from the lithium target in the case of 1 mA current, and from the tungsten target (e, γ) reaction at 1 mA current. Here, the γ -rays of 429 keV and 478 keV are caused by the capture and the inelastic scattering of protons with ${}^7\text{Li}$ respectively and the dependence of their yields on the proton energy were measured; [7] the γ -rays of 14 MeV that may dominate the surface photon dose are produced by the resonance capture of protons by ${}^7\text{Li}$ and their yields have not been measured and roughly estimated; [8] the yield of the Bremsstrahlung case was calculated by the MCNPX.

Table 1 Energies and yields of photons from the ${}^7\text{Li}(p, n)$ target with $E_p = 2.5\text{MeV}$ and the Bremsstrahlung target with $E_e = 35\text{MeV}$ driven by 1 mA current

Reactions of photon production	${}^7\text{Li} (p, n\gamma) {}^7\text{Be}$	${}^7\text{Li} (p, p\gamma) {}^7\text{Li}$	${}^7\text{Li} (p, \alpha \gamma) {}^4\text{He}$	Bremsstrahlung
Energy of photons [MeV]	0.429	0.478	14	Continuous spectrum
Photon yield [1/s]	4.1×10^{10}	2.1×10^{11}	5.7×10^6	1.051×10^{16}

3. Results and discussions

3.1. Neutronic performance

Table 2 summarizes the optimal dimensions of the moderator, the pre-moderator and the reflector for the S- and L-types of cold neutron sources based on four types of reactions, *i.e.* ${}^7\text{Li} (p, n)$ caused by 2 MeV protons or 2.5 MeV protons, ${}^9\text{Be} (p, n)$ caused by 11 MeV protons and Bremsstrahlung (γ, n) caused by 35 MeV electrons. The values given in Table 2 are estimated by the simplified models as shown in Fig. 4 so as to maximize the intensity of cold neutrons less than 5meV. The smaller size of the reflector for the S-type is achieved by the ${}^7\text{Li} (p, n)$ reactions rather than the ${}^9\text{Be} (p, n)$ and the Bremsstrahlung (γ, n) reactions and this may be brought by the smaller energies of neutrons from the ${}^7\text{Li} (p, n)$ reactions than those of the ${}^9\text{Be} (p, n)$ and the Bremsstrahlung (γ, n) reactions as shown in Fig. 5.

Table 2 Optimal dimensions of the moderator, pre-moderator and reflector for various cases of cold neutron sources

Type of source		The moderator thickness [cm]	The pre-moderator thickness [cm]	The reflector thickness [cm]
${}^7\text{Li}(p, n), E_p=2\text{MeV}$	S-type	2.5	1.5	40
	L-type	3.0	1.0	50
${}^7\text{Li}(p, n), E_p=2.5\text{MeV}$	S-type	2.5	1.5	40
	L-type	3.0	1.0	50
${}^9\text{Be}(p, n), E_p=11\text{MeV}$	S-type	2.5	1.5	50
	L-type	2.5	1.0	50
Bremsstrahlung (γ, n), $E_e=35\text{MeV}$	S-type	2.5	1.0	50
	L-type	2.5	1.0	60

Figure 7 shows the comparison of neutron flux spectra per neutron production between the four models, *i.e.* the simplified S-type, the simplified L-type, the S-type and the L-type

of the ${}^7\text{Li}$ (p, n) cold neutron source with 2.5 MeV protons. The neutron spectrum for the L-type shows a steeper inclination above 0.5eV than that of the S-type and almost corresponds to the one-over-E-type slowing down distribution that is represented by the dashed line; this may be caused by that the moderator of the L-type slows neutrons down more efficiently than the S-type since the yield of neutrons from the Li target peaks in the angle of 40 degree to the direction of the initial protons and the thickness of methane in the direction of the initial protons for the L-type is larger than that of the S-type. Consequently the intensity of the neutron flux above 0.5eV or less than 5meV for the L-type becomes 0.5 times or 0.9 times those for the S-type, respectively. Such differences between the S-type and the L-type are not noticeable in the case of the simplified models where the intensity of the neutron flux below 100keV for the L-type moderator is 0.8 times that for the S-type moderator; this may be due to the fact that the neutronic characteristics of the simplified models are not very dependent on the anisotropic neutron productions of the ${}^7\text{Li}$ (p, n) reactions, since in the calculations of the simplified models the Li target is installed on the surface of the pre-moderator and the distance from the Li target to the moderator is short, which is 1.5 cm for the S-type and 1 cm for the L-type.

Figure 8 shows the comparison of neutron flux spectra per neutron production between the ${}^7\text{Li}$ (p, n) cold neutron sources with 2.5 MeV protons and the Bremsstrahlung (γ , n) cold neutron sources with 35 MeV electrons. The intensity of cold neutrons with the energies less than 5meV for the ${}^7\text{Li}$ (p, n) sources are 1.4 times larger than that for the Bremsstrahlung (γ , n) sources, since a part of the high energy neutrons from the Bremsstrahlung (γ , n) target passes by the moderator and does not contribute to the production of cold neutrons at the moderators. Moreover, the curves show the larger difference in the inclination above 0.5eV between the S-type and the L-type of the ${}^7\text{Li}$ (p, n) sources than those of the Bremsstrahlung (γ , n) sources; this may be attributed to the difference in the angular distribution of neutrons between the ${}^7\text{Li}$ (p, n) target and the Bremsstrahlung (γ , n) target as shown in Fig.6.

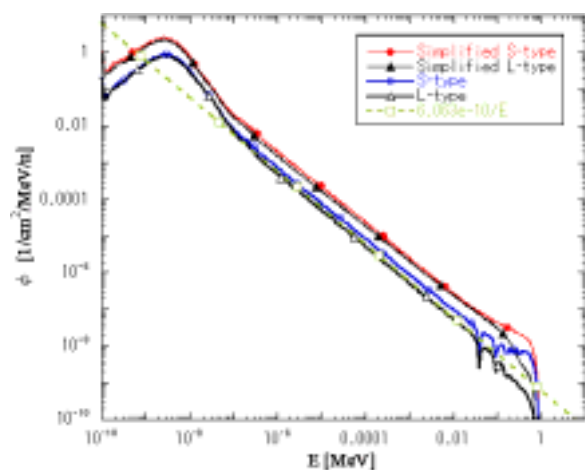


Fig. 7 Comparison of neutron spectra per neutron production at 5 m position between the S- and the L-type ${}^7\text{Li}$ (p, n) cold neutron sources driven by 2.5MeV protons

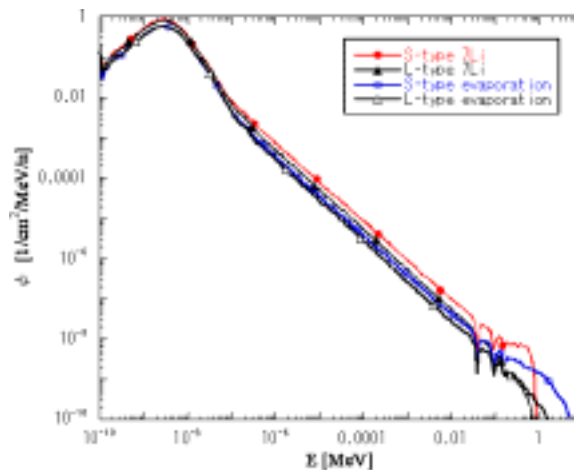


Fig. 8 Comparison of neutron spectra per neutron production at 5 m position between the ${}^7\text{Li}$ (p, n) and the Bremsstrahlung (γ , n) cold neutron sources

Table 3 summarizes the cold neutron fluxes per neutron production for ${}^7\text{Li}$ (p, n) cold neutron source driven by 2.5 MeV protons. The intensity of cold neutrons having the energy less than 5meV for the S-type and the L-type become about 0.4 times those for the

ICANS XIX,
19th meeting on Collaboration of Advanced Neutron Sources
 March 8 – 12, 2010
 Grindelwald, Switzerland

simplified models. This is caused by the shorter distances from the Li target to the moderator, and neglect of the structure materials and the neutron streaming in the channels around the moderator.

Table 3 Comparison between the cold neutron fluxes per neutron production for ${}^7\text{Li}$ (p, n) cold neutron source driven by 2.5 MeV protons

	Neutron flux ($E < 5\text{meV}$) [$1/\text{cm}^2/\text{n}_p$]	Ratio of neutron flux ($E < 5\text{meV}/$ total)	Neutron flux at 5m from a moderator ($E < 5\text{meV}$) [$1/\text{cm}^2/\text{s/kW}$]	Neutron flux at 5m from a moderator ($E < 5\text{meV}$) [$1/\text{cm}^2/\text{s/mA}$]	Ratio of cold neutron flux to simplified model [-]
Simplified S-type	8.63×10^{-3}	0.148	3.04×10^4	7.59×10^4	1
Simplified L-type	7.26×10^{-3}	0.169	2.56×10^4	6.39×10^4	1
S-type	2.92×10^{-3}	0.140	1.03×10^4	2.57×10^4	0.338
L-type	2.66×10^{-3}	0.196	9.36×10^3	2.34×10^4	0.366

Table 4 summarizes the fast neutron yield from a target, the average neutron energy from a target, the neutron fluxes and the conversion ratio to the cold neutrons for the sources with various reactions. The fast neutron yield from the target increases with the energy of the initial particles. The conversion ratio to the cold neutrons, that is the cold neutron flux per fast neutron production, decreases with the increase in the average energy of neutrons from the target. This is again brought by the smaller energies of neutrons from the ${}^7\text{Li}$ (p, n) reactions than the ${}^9\text{Be}$ (p, n) and the Bremsstrahlung (γ , n) reactions. Considering the bombardment of the lithium foil by protons with an energy of 2.5 MeV and a current of 1 mA yields neutrons of $8.8 \times 10^{11} \text{ s}^{-1}$, it is estimated that the L-type of the ${}^7\text{Li}$ (p, n) cold neutron source of 2.5 KW ($E_p=2.5\text{MeV}$, $I=1\text{mA}$) produces the intensity of cold neutrons with the energy of less than 5 meV of $2.34 \times 10^4 \text{ cm}^{-2} \text{ s}^{-1}$ at 5 meter from the moderator, which corresponds to that for the Bremsstrahlung (γ , n) cold neutron source of 0.77 KW ($E_e=35\text{MeV}$, $I=0.022\text{mA}$). For the comparison of shields, we adopted this power of Bremsstrahlung reaction.

Table 4 Fast neutron yield from a target, the average neutron energy from a target, the neutron fluxes and the conversion ratio to the cold neutrons for the sources with various reactions

Type of source		Fast neutron yield from a target [$\text{n}_p/\text{s/kW}$]	Fast neutron yield from a target [$\text{n}_p/\text{s/mA}$]	Average neutron energy from a target [MeV]	Neutron flux at 5m from a moderator ($E < 5\text{meV}$) [$1/\text{cm}^2/\text{s/kW}$]	Neutron flux at 5m from a moderator ($E < 10\text{meV}$) [$1/\text{cm}^2/\text{s/kW}$]	Neutron flux at 5m from a moderator ($E < 5\text{meV}$) [$1/\text{cm}^2/\text{s/mA}$]	Neutron flux at 5m from a moderator ($E < 10\text{meV}$) [$1/\text{cm}^2/\text{s/mA}$]	Conversion ratio to cold neutrons ($E < 5\text{meV}$) [$1/\text{cm}^2/\text{n}_p$]
${}^7\text{Li}$ (p, n), $E_p=2\text{MeV}$	S-type	5.50×10^{10}	1.10×10^{11}	0.075	1.93×10^3	3.21×10^3	3.85×10^3	6.42×10^3	3.50×10^{-8}
	L-type				1.66×10^3	2.79×10^3	3.32×10^3	5.59×10^3	3.02×10^{-8}
${}^7\text{Li}$ (p, n), $E_p=2.5\text{MeV}$	S-type	3.52×10^{11}	8.80×10^{11}	0.326	1.03×10^4	1.73×10^4	2.57×10^4	4.32×10^4	2.92×10^{-8}
	L-type				9.36×10^3	1.58×10^4	2.34×10^4	3.94×10^4	2.66×10^{-8}
${}^9\text{Be}$ (p, n), $E_p=11\text{MeV}$	S-type	1.95×10^{12}	2.15×10^{13}	2.04	4.20×10^4	7.13×10^4	4.62×10^5	7.85×10^5	2.15×10^{-8}
	L-type				4.05×10^4	6.96×10^4	4.45×10^5	7.65×10^5	2.07×10^{-8}
Bremsstrahlung (γ , n), $E_e=35\text{MeV}$	S-type	1.60×10^{12}	5.60×10^{13}	2.52	3.25×10^4	5.54×10^4	1.14×10^6	1.94×10^6	2.03×10^{-8}
	L-type				3.07×10^4	5.30×10^4	1.08×10^6	1.85×10^6	1.92×10^{-8}

3.2. Design for the shielding components

a) Necessary thickness of the shield for γ -rays

Figure 9 shows the calculation model for examining the necessary thickness of the shield around the source, in the case of the S-type of the ^7Li (p, n) cold neutron source of 2.5 KW ($E_p=2.5\text{MeV}$, $I=1\text{mA}$). For the shielding components for γ -rays, the lead slabs or the iron slabs are installed on the all surfaces of the reflector. The case of the Bremsstrahlung (γ , n) cold neutron source of 0.77 KW ($E_e=35\text{MeV}$, $I=0.022\text{mA}$) was also examined for comparison, where the lead slabs or the boron-enriched concrete slabs are installed on the all surfaces of the reflector. The photon dose distributions on the slabs with various thicknesses were calculated.

Figure 10 shows the maximum photon dose on the shielding components depending on the thickness of the slab. The 12 cm thick lead slab and the 24 cm thick iron slab decrease the surface photon dose on the shield to $20 \mu\text{Sv/h}$ in the case of the ^7Li (p, n) cold neutron source of 2.5 KW. The use of iron as a substitute for lead increases the weight of all the slabs from 13.3 ton to 22.1 ton. These results show that it is better to use the lead slab shields for the ^7Li (p, n) cold neutron source of 2.5 KW.

Next, we consider the case of the Bremsstrahlung. The 34 cm thick lead slab and the 260 cm thick boron-enriched concrete slab decrease the surface photon dose on the shield to 1 mSv/h in the case of the Bremsstrahlung (γ , n) cold neutron source of 0.77 KW. The thicker lead slab necessary for the Bremsstrahlung reaction than the ^7Li (p, n) reaction is caused by that the Bremsstrahlung by electrons of 0.77 KW not only yields much more photons $2.31 \times 10^{14} \text{ s}^{-1}$ than the ^7Li (p, n) by protons of 2.5 KW $2.51 \times 10^{11} \text{ s}^{-1}$ but also contains the more energetic photons than the ^7Li (p, n) by protons of 2.5 KW.

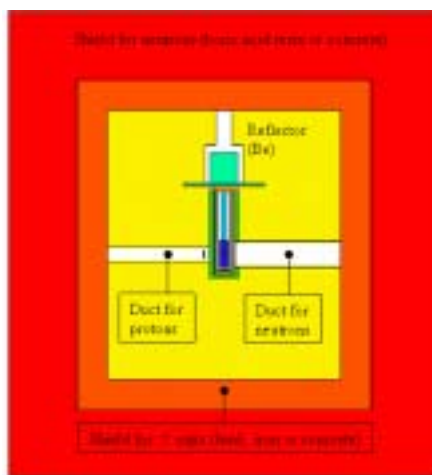


Fig. 9 Longitudinal section of the calculation model for examining the thickness of the shield around the S-type source

b) Necessary thickness of the shield for neutrons

The boric acid resin slabs are installed on the all surfaces of the 12 cm thick lead slabs as in Fig. 9. The neutron dose distributions on the boric acid resin slabs with various thickness were calculated. The case where the boron-enriched concrete slabs are installed on the all surfaces of the 12 cm thick lead slabs was also examined for comparison. We also examined the case of the Bremsstrahlung (γ , n) cold neutron source of 0.77 KW.

Figure 11 shows the maximum neutron dose on the shielding components depending on the thickness of the slab. The 30 cm thick boric acid resin slab and the 40 cm thick boron-enriched concrete slab decrease the surface neutron dose on the shield to 10 $\mu\text{Sv/h}$ in the case of the ^7Li (p, n) cold neutron source of 2.5 KW. The thicker concrete slab than the boric acid resin slab is caused by that the density of hydrogen ($2.49 \times 10^{22} \text{ cm}^{-3}$) and boron ($1.54 \times 10^{21} \text{ cm}^{-3}$) in the boron-enriched concrete are smaller than those of the boric acid resin, which are $4.71 \times 10^{22} \text{ cm}^{-3}$ and $9.04 \times 10^{21} \text{ cm}^{-3}$ respectively. The difference between the thickness of the boric acid resin slabs and that of the boron-enriched concrete slabs may be small; however, the use of the boric acid resin as a substitute for the boron-enriched concrete can decrease the weight of all the slabs from 17.2 ton to 6.9 ton and may make the construction cost for the shield decrease.

The 120 cm thick boric acid resin slab and the 130 cm thick boron-enriched concrete slab decrease the surface neutron dose on the shield to 10 $\mu\text{Sv/h}$ in the case of the Bremsstrahlung (γ , n) cold neutron source of 0.77 KW. Since the fast neutron yield from the Bremsstrahlung (γ , n) target of 0.77 KW $1.23 \times 10^{12} \text{ s}^{-1}$ does not differ widely from that of the ^7Li (p, n) target of 2.5 KW $8.80 \times 10^{11} \text{ s}^{-1}$, the thicker shielding necessary for the Bremsstrahlung (γ , n) cold neutron source than the ^7Li (p, n) cold neutron source is attributed to the neutrons with energies more than 800 keV emitted from the Bremsstrahlung (γ , n) target of 0.77 KW.

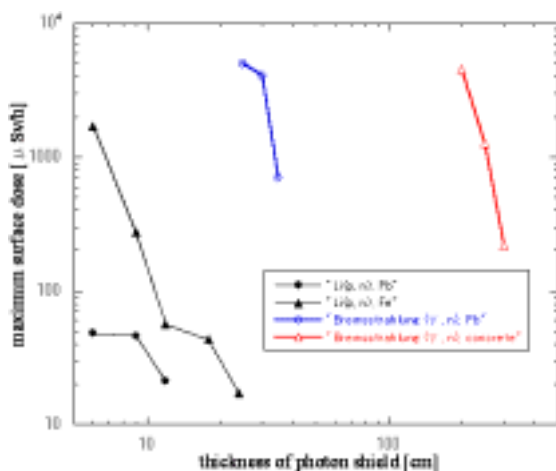


Fig. 10 Dependence of the maximum photon dose on the thickness of the slabs

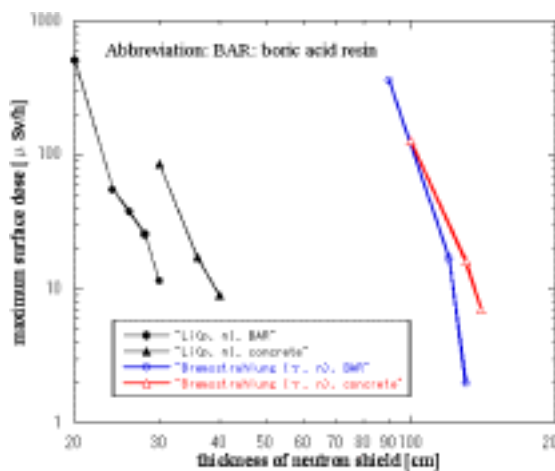


Fig. 11 Dependence of the maximum neutron dose on the thickness of the slabs

c) Whole of shielding components for photons and neutrons

We further designed the shields around the sample for scattering experiments, the duct for neutrons and the proton liner accelerator. It turned out that a 42 cm thick radiation shield consisting of a 12cm thick inside lead slab and a 30 cm thick outside boric acid resin slab, which is identical to that around the cold neutron source mentioned above, is adequate to reduce the surface radiation dose on the shields down to 20 $\mu\text{Sv/h}$.

4. Conclusions

ICANS XIX,
19th meeting on Collaboration of Advanced Neutron Sources
March 8 – 12, 2010
Grindelwald, Switzerland

We have examined the performance of models for a cold neutron source equipped with a Li target and a proton linear accelerator with the proton energy of 2.5MeV and the beam current of 1mA. We also studied the Bremsstrahlung (γ , n) cold neutron sources to reveal the effects of the energy and angular distributions of source neutrons on the neutron fluxes. It turned out that the neutron flux spectra of the ^7Li (p, n) cold neutron source are dominated by the anisotropic neutron productions of the Li target. Further, the intensity of cold neutron flux per neutron production for the ^7Li (p, n) sources were 1.4 times larger than that of the Bremsstrahlung (γ , n) sources, since a part of the high energy neutrons from the Bremsstrahlung (γ , n) target passes by the moderator and does not contribute to the production of cold neutrons at the moderators. It turned out that the ^7Li (p, n) cold neutron source of 2.5 KW produces the cold neutrons corresponding to a Bremsstrahlung (γ , n) cold neutron source of 0.77 KW.

For reducing the volume of shields for the ^7Li (p, n) cold neutron source of 2.5 KW, we adopted shields with two layers consisting of the inside lead slabs for the photons and the outside boric acid resin slabs for the neutrons. It turned out that the ^7Li (p, n) cold neutron source of 2.5 KW needs a much smaller volume of the shielding components than those for typical Bremsstrahlung (γ , n) cold neutron sources of 0.77 KW. These results indicate that a very compact cold neutron source will be realized by using the ^7Li (p, n) reaction.

5. References

1. <http://www.accsys.com/products/lansar.html>
2. T. Tadokoro, *et al.*, “*The Feasibility Study of the Boron Neutron Capture Therapy Using Proton Linac— Including the Isotope Generation for the PET Diagnosis—*,” The 2nd Meeting of Particle Accelerator Society of Japan (2005), [in Japanese]
3. C.L. Lee, X.-L. Zhou, Nucl. Instr. Meth. B 152, 1 (1999)
4. J. F. Briesmeister (ed.), *MCNP_A General Monte Carlo N-Particle Transport Code, Version4A*, LA-12625, (1993)
5. S. Kamada, *et al.*, Preprints 2006 Spring Meeting of At. Energy Soc. Jpn., K42, (2006), [in Japanese]
6. K. Okuno, *et al.*, Nucl. Technol. 168, 545 (2009)
7. A. Z. Kiss, *et al.*, J. Radioanal. Chem. 89, 123 (1984)
8. C.L. Lee, X.-L. Zhou, *et al.*, Med. Phys. 27, 192 (2000)